Full Title: Predicting Vertical Ground Reaction Force During Running Using Novel Piezoresponsive Sensors and Accelerometry

Running Title: Novel Sensors to Predict Running Ground Reaction Force

Key Words: wearables, gait, biomechanics

Authors: Matthew K. Seeley[1], Alyssa E. Pickett[1], Gavin Collins[2], James Tracy[1], Noelle Tuttle[1], Parker Rosquist[3], Jake Merrell[3], William F. Christensen[2], David Fullwood[3], and Anton E. Bowden[3]

Departments of Exercise Sciences[1], Statistics[2], and Mechanical Engineering[3], at Brigham Young University, Provo, UT, USA

Abstract (196 Words)

Running is a common exercise with numerous health benefits. Vertical ground reaction force (vGRF) influences running injury risk and running performance. Measurement of vGRF during running is now primarily constrained to a laboratory setting. The purpose of this study was to evaluate a new approach to measuring vGRF during running. This approach can be used outside of the laboratory and involves running shoes instrumented with novel piezoresponsive sensors and a standard accelerometer. Thirty one individuals ran at three different speeds on a force-instrumented treadmill while wearing the instrumented running shoes. vGRF were predicted using data collected from the instrumented shoes, and predicted vGRF were compared to vGRF measured via the treadmill. Percent error of the resulting predictions varied depending upon the predicted vGRF characteristic. Percent error was relatively low for predicted vGRF impulse (2-7%), active peak vGRF (3-7%), and ground contact time (3-6%), but relatively high for predicted vGRF load rates (22-29%). These errors should decrease with future iterations of the instrumented shoes and collection of additional data from a more diverse sample. The novel technology described herein might become a feasible way to collect large amounts of vGRF data outside of the traditional biomechanics laboratory.

Introduction (Total Word Count = 5380)

Scientists have estimated that 64 million Americans run for exercise, and more than 30,000 official running races were held in 2017 [1]. Multiple salutary health benefits result from running [2]. For example, when combined with appropriate nutrition, running for exercise can improve cardiovascular health [3], increase skeletal strength [4], and enhance cognitive performance [5]. Distance running may even maintain or improve joint health for young healthy individuals [6]. Wearable devices can provide important information concerning an individual's health status and increase an individual's motivation to exercise, including running [7-9].

Vertical ground reaction force (vGRF) applied to the plantar surface of the foot during running strongly influences magnitude of load transmitted through lower-extremity joints, including the ankle, knee, and hip. Specific characteristics of vGRF during running are associated with musculoskeletal injury etiologies, joint disease progression rates, and athletic performance. For example, peak vGRF magnitude during sprinting (i.e., the active peak; Figure 1) is related to speed and corresponding performance [10], as well as risk for various musculoskeletal injuries during running [11-13]. Impact peak vGRF and corresponding load application rate (Figure 1) have also been associated with musculoskeletal injury risk; numerous researchers have hypothesized that running injury risk increases as peak impact vGRF and corresponding load rate increase [14-19]. Duration of the foot-ground contact phase of running (Figure 1) has also been associated with running performance: increased ground contact duration corresponds to decreased running speed [10, 20-22] and increased fatigue [23]. Impulse due to vGRF (the time integral of the vGRF during the ground contact phase) is a measure that simultaneously considers vGRF magnitude and ground contact time. This impulse, and measures

derived from it, are thought to influence running performance [24, 25] and risk of joint injury and disease [24, 26].

Although vGRF magnitude and other characteristics are valuable to consider during running, high cost and limited mobility of force platforms now limit accurate measurement of vGRF to traditional biomechanics research laboratories. Further, certain characteristics of running vGRF measured inside a traditional motion analysis laboratory likely differ from the same characteristics of running vGRF measured outside of the laboratory [27-30]. Additionally, without an expensive force instrumented treadmill, it is difficult to collect a substantial number of laboratory running trials. Researchers are currently seeking ways to measure vGRF outside of the laboratory, recently testing effectiveness of various novel approaches, like accelerometry [31, 32], inertial measurement units [31, 33, 34], and different measures of plantar pressure [35-38]. In particular, the capability of inertial measurement units to estimate continuous 3D ground reaction force traces, during various human movements has been evaluated, via direct modeling methods and machine learning methods [31], with varying levels of success.

The purpose of the present project was to test the accuracy of a new sensing technology, different from inertial measurements, in predicting important characteristics of vGRF during running at three different speeds. This new technology is an inexpensive nanocomposite piezoresponsive foam (NCPF) that can be inserted into the running shoe under the insole (Figure 2). When the NCPF is compressed, conductive additives in the foam interact with the foam substrate, creating a triboelectric response that is related to the vGRF applied to the plantar surface of the foot. Rather than measuring inertial properties on externally fixed devices, as accelerometers and inertial measurement units do, this new technology directly measures ground reaction forces at the foot-ground interface. The capability of accurately predicting the following

discrete vGRF characteristics, using the new technology, was evaluated: (1) active and impact peak vGRF magnitudes, (2) average and maximum instantaneous load rates for the impact peak vGRF, (3) impulse due to vGRF during the ground contact phase, and (4) duration of the ground contact phase. The capability of determining heel strike pattern was also evaluated; i.e., whether test subjects ran with a heel strike or non-heel strike pattern. This was evaluated because this is a running characteristic that has also been hypothesized to be related to running injury rates [39, 40]. Prior to this study, it was unknown whether the new NCPF technology could be used to accurately measure vGRF during running.

Methods

Subjects

Thirty one volunteers (17 male, 14 female; age = 23 ± 3 years; mass = 68 ± 10 kg; height = 174.4 ± 8.0 cm) participated in this study. Subjects were required to be between the ages of 18 and 30, have no lower-extremity injury within six months of data collection, and have no history of lower-extremity surgery. All subjects reported that they could continuously run for at least 5 km at each of the tested running speeds. Due to a limited number of instrumented shoes at the time of data collection, subjects were required to wear one of the following U.S. shoe sizes: 9.5, 10.5, or 11.5 for male subjects, or 7, 8, or 9 for female subjects. Subjects provided informed consent before data collection. All procedures were approved by the appropriate institutional review board.

Instrumentation

Subjects wore standardized athletic shoes. For each subject, the right shoe was instrumented with the novel NCPF sensors (under the insole) and an accelerometer (Range = ± 16 g's; Bosch Sensortec, Mount Prospect, IL, USA) for all of the running trials (Figure 2). The same instrumented shoes were worn during previous experiments designed to predict continuous vGRF during walking [41]. The NCPF sensors are made of a combination of nickel coated nano carbon fibers and dendritic nickel powder, added to a polyurethane foam substrate. When the NCPF sensors are compressed during running, conductive additives in the foam interact with the foam substrate to create a triboelectric response. This electrical response is measured by embedding a conductive material into the foam attached to a voltage measurement system. The measured voltages are associated, as described later in this manuscript, with the vGRF. The NCPF sensors were positioned under the shoe insole, in locations generally corresponding to the

heel, arch, ball, and great toe of the foot (Figure 2). Each subject's right shoe was also instrumented with a microcontroller to collect voltage response data from the NCPF sensors and accelerometer; these voltage data were stored on a MicroSD card and uploaded after each data collection session. A reflective marker was placed on both the right and left shoe, posterior to the heel, over the 2nd distal phalanx, and over the head of the 5th metatarsal; these markers and high-speed video (VICON, Centennial, CO, USA) were used to measure the motions of the right and left feet during running. This motion analysis was used only to assign the vGRFs to the correct foot (right or left). Only vGRF applied to the instrumented foot were analyzed during the present study. A force instrumented treadmill (AMTI, Watertown, MA, USA) was used to measure actual vGRF, including ground contact time which was necessary to evaluate accuracy of the predicted vGRF characteristics.

Data Collection Procedures

While wearing the aforementioned standardized running shoes, subjects first performed a 15 minute warmup run on the force instrumented treadmill at a speed of 2.68 m/s. Subjects were then instructed to ambulate (walk or run) at the following speeds for four minutes each: 2.24, 2.68, 3.13, and 3.58 m/s. Only data collected at the three fastest speeds were presently analyzed because these speeds represented actual running gait for all of the subjects: several subjects chose to walk quickly at the slowest speed, determined from the observation of a double-limb support phase. Throughout each 4-minute running session, data were continuously collected from the NCPF sensors (1029 Hz), accelerometer (16 Hz), instrumented force treadmill (1000 Hz), and high-speed video cameras (250 Hz). At the beginning of each running speed, subjects stomped on the instrumented treadmill. This stomp/event was used to synchronize the NCPF sensor, accelerometer, treadmill, and video data. The NCPF sensor, accelerometer, and video

data were all resampled to 1000 Hz so that all data could be synchronized to the vGRF data collected using the instrumented treadmill. Additionally, the NCPF sensor and vGRF data were filtered via a 4^{th} order Butterworth filter with a low-pass cutoff frequency of 75 Hz. Due to two different errors in the data collection process, data were unavailable for the 3.13 and 3.58 m/s speeds for one subject and for the 3.58 m/s speed for two other subjects: battery failure in the instrumented shoes for one subject and two subjects were unable to complete the fastest speed. Ultimately, for all subjects combined, 9924, 9666, and 9131 running strides (defined as initial ground contact to subsequent initial ground contact) were collected for the 2.68, 3.13, and 3.58 m/s running speeds, respectively. Representative vGRF traces measured using the instrumented treadmill are shown for three different subjects in Figure 3.

Variable Definitions and Data Reduction

Impact peak vGRF was defined using a previously described approach [42]; essentially, impact peak was identified when impact peak was at least 1.2 times greater than a subsequent local minimum vGRF, early in the ground contact phase. Active peak vGRF was defined as maximum vGRF during each running stride. Impulse was defined as the time integral of vGRF during each running stride. Ground contact duration was defined as the duration of vGRF application during each running stride. All of these quantities are depicted in Figure 1. Ground contact phases containing an impact peak were considered to represent a heel-strike pattern, while ground contact phases with no impact peak were considered to represent a non-heel strike pattern. Maximum instantaneous impact peak load rate was defined as the maximum time derivative of vGRF between initial ground contact and impact peak. Average impact peak load rate was defined as the average rate of vGRF change between initial ground contact and impact

peak. Impact peak vGRF magnitude, maximum instantaneous impact peak load rate, and average impact peak load rate were analyzed only for running strides exhibiting a heel-strike pattern.

The beginning and end of each running stride were identified using the accelerometer data because this will be necessary when the instrumented shoe is used outside the laboratory. After experimenting with several different approaches, the following approach was chosen because it matched well with the beginning and end of each running stride, as determined using the instrumented treadmill (touchdown and toeoff were defined as the time vGRF increased to above 50 N and then decreased below 50 N, respectively). Initial ground contact was defined to occur 65 ms prior to peak acceleration in the Z direction for each running stride. The accelerometer was consistently positioned and oriented so that the Z axis was most closely aligned to vertical, while the foot was flat on the ground, with the subject in a static standing position.

In total, 54 potential predictor variables were available to predict the running vGRF characteristics of interest. These variables are described in this paragraph. For each observed running stride, certain discrete characteristics of eight signals were used, including the three orthogonal components of acceleration and resultant acceleration, measured using the accelerometer, and one signal from each of the four NCPF sensors (Figure 2). Six potentially predictive characteristics of these eight signals were identified: absolute maximum, absolute minimum, time to absolute maximum, time to absolute minimum, time integral, and primary signal frequency. Additionally, six other characteristics were available to predict characteristics of the running vGRF: (1) running stride duration derived from the acceleration data (for each observed running strides), (2) subject age, (3) subject gender, (4) subject height, (5) subject weight, and (6) subject body mass index (BMI).

Statistical Analysis

To create statistical models capable of accurately predicting discrete vGRF characteristics, two potential prediction approaches were considered. First, a unique statistical model was created for each subject to produce vGRF predictions as accurate as possible for each subject. This approach in practice required a separate calibrated model for each subject, necessitating methods described in this paper for every individual end user. Second, a general model encompassing all of the present subjects; while predictive accuracy is sure to be less using this approach, no calibration is required before vGRF predictions can be made for any end user within the involved demographic range. The first approach might be more appropriate for researchers who have access to the data collection and analytical tools described in this paper, while the second approach is likely more realistic in a commercial setting where a subject-specific lab calibration process is not feasible. In this subsection, the process of building a general model is first described for all of the present subjects and then the process is extended to create subject-specific models.

The general model was created to predict vGRF characteristics for subjects that are similar to the present subjects. The response variables of interest were impact peak, instantaneous and average load rates, active peak, impulse, and ground contact duration. For each of these variables of interest, the 54 potential predictor variables were ordered in terms of their ability to represent the response. This ordering was done by representing the response with a linear regression model, and then conducting a forward selection process with the sum of squared residuals as the selection criterion. Backward selection and sequential replacement/stepwise selections were also tried, but forward selection yielded optimal results. For a more complete discussion of the model selection process, see Section 9.4 of Kutner et al.

193 [43]. This yielded a total of 54 potential models, the first including only the most important
194 predictor variable, the second including the two most important variables, etc. It's well-known
195 that variable selection procedures based on in-sample data tend to overfit the data and produce
196 less-than-optimal out-of-sample predictions [44]. So in order to determine which of these 54
197 models would provide the most accurate out-of-sample predictions, a leave-one-subject-out
198 cross-validation process was performed (Section 5.1 of [45]) and the model that yielded the
199 lowest cross-validated root mean square error (RMSE), averaged across all subjects, was
200 selected; i.e., the selected model was the one that most accurately predicted a single excluded
201 subject's vGRF characteristics. Corresponding percent errors were also calculated, defined as the
202 ratio $\frac{|actual-predicted|}{actual} \times 100\%$. The predictor variables were also used to obtain stride-by-stride
203 predictions of foot-strike pattern, classified as either heel-strike or non-heel-strike. The process
204 for selecting the optimal model for heel-strike pattern identification was identical to the process
205 for the other six variables, except that logistic regression was used in place of standard linear
206 regression, and error was measured in terms of the percentage of misclassified strides, rather than
207 RMSE.
208 Some of the selected models contained predictors that are highly correlated with one
209 another; e.g. subject weight and BMI in the vGRF, impulse, and ground contact time models. In
210 order to alleviate concerns with multi-collinearity, coefficient estimation and inference for all
211 models were performed using principal component regression (PCR) on the selected variables.
212 PCR is a simple extension of multiple regression that replaces the original matrix of predictor
213 variables (**X**) with a new matrix of predictors **Z**, where **Z**=**XC** and **C** contains the subset
214 of *m* eigenvectors of **X**′**X** that correspond to the *m* largest eigenvalues of **X**′**X**. Although we
215 estimate the regression coefficients associated with the new predictors in **Z**, we are easily able to

transform these coefficients back to the scale of the original variables in **X** for simple interpretation. For a thorough discussion of PCR, see either of the following two references [46, 47]. Furthermore, the usual regression assumption of independent residuals is clearly invalid here, as we expect substantial correlation between observations within a trial, especially for observations that are close together in time. To account for this, we included a random intercept, and modeled the residuals with an AR(1) structure, for each subject-trial combination. For further details on random effects see the following reference [48].

This process was then extended to select optimal models of the response variables for each of the 30 subjects. Because these models were independent across subjects, the five demographic variables were not utilized in this process. Further, because the dataset for each subject was much smaller than the entire dataset, it was necessary to exclude some predictor variables, including the eight primary frequency variables; i.e., primary frequencies of the signals originating from the NCPF sensors and accelerometer. Thus, there were 41 potential predictor variables here. The variables were ordered using data from all 30 subjects, just as in the ordering process for creating the general model, yielding a total of 41 potential models. Instead of performing a leave-one-subject-out cross-validation process using data from all subjects, a separate cross-validation process was performed for each subject, treating the first 50% of the strides from each of the three running speeds as the training set and the remaining strides as the test set. The final set of common predictor variables for the subject-specific models was the one that minimized the average cross-validation error across all subjects, measured by RMSE for the quantitative variables and misclassification rate for foot-strike pattern. As with the general model, the final subject-specific models were fit using principal components regression, with a random intercept term and an AR(1) component to account for within-trial correlation. To

239 evaluate the predictive ability of these models, final cross-validation analyses were run where
240 30%, 50%, and 70% of each subject's data were used as training data to better understand the
241 amount of data needed to create an accurate subject-specific model.

Results

Descriptive statistics for the vGRF characteristics of interest, measured using the force instrumented treadmill, are presented in Table 1. Initially, to explore our entire data set prior to the construction of the prediction models described in the methods section, we calculated Pearson correlation coefficients between each potential predictor variable, including characteristics of the NCPF sensors, accelerometer, and subject demographics, and the vGRF characteristics of interest (Table 2). Many of these correlations indicated a moderate-to-strong association between the potential predictors and vGRF characteristics of interest. Consequently, we anticipated that a statistical model based on these predictors would be at least moderately successful in predicting characteristics of vGRF during running.

After performing the aforementioned initial correlational analyses, we constructed predictive models for each vGRF characteristic of interest using the predictor-subset-selection approach described in the methods section. Average RMSE from the leave-one-subject-out cross-validation analyses of the general across-all-subjects models are presented in Table 3, along with the corresponding percent error. Figure 4 shows predicted values from these general models, plotted against the corresponding actual, measured values. RMSE for active peak vGRF magnitude, impulse due to vGRF, and ground contact duration were lower, relative to the RMSE for the other predicted vGRF characteristics. RMSE for impact peak vGRF, and the average and maximum instantaneous load rates were relatively high. Bias is near zero for all variables, as shown in Figure 4. Additionally, using the general approach, across-all-subjects, 66.1% of the running strides were correctly identified as either a heel-strike or non-heel-strike pattern; 65.1% and 67.8% of the heel-strike and non-heel-strike patterns, respectively, were identified correctly. Appendix A shows the predictor variables included in the final across-all-subjects model for

each quantitative vGRF characteristic and foot-strike pattern identification. For example, the general model for average impact rate is:

$$Average\ Impact\ Rate = \beta_0 + \beta_1 TimeInt_Z^* + \beta_2 Max_{Heel}^* + \beta_3 Min_{Heel}^* + \beta_4 Max_{Ball}^* + \beta_5 Min_{Ball}^* + \beta_6 TimeInt_{Ball}^* + \beta_7 Weight^*,$$

where x^* is the standardized version of variable x, e.g. $TimeInt_Z^* = \frac{TimeInt_Z - mean(TimeInt_Z)}{sd(TimeInt_Z)}$.

Among all models, subject weight was the most commonly selected variable. Age was used only in the ground contact time model. Variables derived from acceleration in the X direction, which was approximately in the anterior-posterior direction, were not commonly selected compared to other accelerometer variables. Variables derived from the arch and toe sensors were selected less often than variables derived from the heel and ball sensors. Some common regression statistics further describing the final across-all-subjects models (Table 3) are presented in Appendix B.

Average RMSE, along with corresponding percent error, for the cross validation analyses of subject-specific models is contained in Table 4. As anticipated, RMSE for the subject-specific models were consistently lower than for the general models. Similar to the results related to the general model, percent error was smallest for active peak vGRF, impulse due to vGRF, and ground contact time, and prediction errors were greater for impact force GRF and maximum instantaneous impact and average load rates. As expected, prediction errors were often greater when only 30% of a subject's running data were used to train the models, relative to using 50% or 70% of a subject's running data (Table 4). Additionally, the existence of a heel-strike pattern was identified much more accurately for the subject-specific models relative to the general model. On average, the subject-specific models correctly identified a heel-strike pattern approximately 87% of the time, and this did not appear to be substantially affected by the amount of training data used: the model accurately identified heel strike 85.5 and 87.8% of the

288 time when the data-usage percentage was 30 and 70%, respectively, of the running strides for the
289 training data.

Discussion

The purpose of this study was to evaluate a new approach involving novel piezoresponsive sensors and statistical modeling methods to predict specific characteristics of vGRF during running. This study was conducted in a traditional biomechanics laboratory, but is a step toward using the evaluated approach to measure vGRF outside of the traditional biomechanics laboratory. The present work is important because running vGRF affects injury risk and performance, and running biomechanics likely differ inside and outside the laboratory [27, 28, 49, 50]. The current results demonstrated that the evaluated approach was satisfactorily accurate in predicting active peak vGRF magnitude, impulse due to vGRF, and ground contact time, especially when using prediction models specific to each individual user, in which case average errors were 2.9, 1.7 and 3.6%, respectively, when using a 50% cross-validation procedure (Table 4). The present approach was less effective in accurately predicting impact peak vGRF magnitude and corresponding average/maximum load rates, with average errors ranging from 9 to nearly 26% in the 50% cross-validation procedure performed on subject-specific models. Future research is required to increase accuracy for all variables, especially predictions of impact peak vGRF and corresponding load rates.

Prediction errors for ground contact time ranged from 11 ms (3.4%) for the most accurate subject-specific model to 17 ms (5.8%) for the general across-subjects model (Tables 3-4). These levels of accuracy are likely sufficient to detect fatigue during distance running; e.g., ground contact time was shown to increase 13.1% between the early and later stages of a marathon [23]. The detection of fatigue is important because fatigue is associated with running performance and various running injuries [51-54]. Further, the presently reported errors for peak active vGRF, which ranged from 59 (2.9%) to 130 N (6.9%; corresponding to the best subject-specific model

and the general across-subjects model, respectively), are also likely acceptable for certain applications. For example, differences in active peak vGRF of about 5% are known to exist between heel-strike and non-heel-strike patterns [55], and differences of about 7.5% are known to exist between a healthy and impaired (chronic ankle instability) subject sample [56]. Conversely, average errors reported herein for predicted average and maximum instantaneous impact load rates are likely not acceptable for any known application. These errors, predicted via both the subject-specific and general models, ranged from approximately 22 to 29%, respectively. In comparison, a recent systematic review concerning potential associations between vGRF load rates and tibial stress fracture, a relatively common running injury, reported an average difference of only 12% in load rate between healthy and injured runners [19]. In speculation, perhaps the present relatively high errors for load rates were due to the high-frequency nature of these signals and low sampling rate of the accelerometer used during the present study. In future iterations of the present system, an upgraded accelerometer will be used, which might improve the accuracy of predictions concerning high frequency characteristics of the vGRF. Accurate predictions of impact vGRF and corresponding load rates is of interest because such predictions can be used to provide biofeedback to runners concerning these variables. Researchers recently reported that biofeedback concerning impact vGRF and load rates, provided in the laboratory, can be used to reduce impact vGRF and corresponding load rates [57]. Such biofeedback might be even more effective when provided for longer durations, outside of the laboratory, although future testing is needed to test this idea.

Two approaches were presently taken to predict running vGRF characteristics: subject-specific models and a general model applicable to all subjects within the demographic range of the current sample. As expected, the subject-specific models were more accurate for every vGRF

characteristic and would be preferred, however, this approach requires a calibration process for each end user. An instrumented treadmill is necessary for this approach, limiting the approach to research settings and/or a small number of clinical settings; although simple predictive variables (e.g., age, height, weight, and gender) were presently required, relative to more complex kinematic measures necessary to derive vGRF from inertial measurement unit data. Regarding the subject-specific models, the use of 70% of the stances as training data generally yielded only a small improvement in accuracy relative to using 50% of the stances as training data. Because it took approximately two minutes of running at each ambulation speed to collect 50% of the stances, we conclude that when creating a subject-specific calibration, predictive accuracy is nearly optimized with just two minutes of data-collection at each speed, or six minutes of total running. The general prediction models were always less accurate than the subject-specific models; however, a potential end user who fits within the demographic range of the present subjects could expect to have errors comparable to errors reported herein. The general prediction models are especially valuable because a new subject can be measured without the creation of a new prediction model. The general prediction models will be necessary to collect data using the present novel sensors on a desirably large scale (e.g., at least thousands of users). Additionally, recruitment and analysis of more subjects will increase the accuracy of the general models. In the future, we plan to use other analytical approaches like machine learning, still in combination with the NCPF sensors and accelerometry, to predict running vGRF characteristics to further improve accuracy of the prediction models.

It is somewhat difficult to compare the present results to previous related research, because few researchers have reported attempts to predict running vGRF characteristics using a single wearable device; additionally, the present NCPF technology is fundamentally different

from previous technologies used to measure ambulatory vGRF. Further, most previous reports concerning wearable devices designed to measure ambulatory vGRF have focused on walking rather than running. The study that is most similar to the present study used one uniaxial accelerometer positioned over the shoe laces and a neural network model to measure impact and active peak vGRF during running at three speeds [32]. Errors for prediction of peak impact vGRF were comparable to the present results and ranged from 0.10 to 0.18 body weights, depending upon running speed; errors for the peak active vGRF ranged from 0.10 to 0.12 body weights. Other researchers have used inertial measurement units placed in various anatomical locations to predict walking, running, and jumping vGRF, with errors comparable to or greater than the present errors [31, 33, 34, 58]. Previous researchers have also used pressure insoles to predict various components of the walking ground reaction force [59-61].

Relatively tight scatter plots for average and max impact rate (Figure 4) could be perceived to indicate greater predictive accuracy, yet greater percent error resulted in the prediction of these two variables (Table 3). This is because percent error $\left(\frac{|actual-predicted|}{actual} \times 100\right)$ naturally decreases with increases in the measured (actual) values. This idea is illustrated by comparing percent error between the impulse (7%) and max impact rate models (25%). Judging using only percent error, the impulse model appears to be more accurate, yet the scatter plots in Figure 4 appear to imply somewhat more accurate predictions of max impact rate. This is partly due to the fact that measures of impulse ranged from 158 to 373 Ns, while measures of max impact rate ranged from 16 to 179 kN/s (Figure 4); i.e., measures of max impact rate clustered relatively closer to zero than measures of impulse. In addition, Figure 4 clearly shows that distinct clusters were prominent for some variables (active peak vGRF and impulse), but not others (average and max impact rate); these clusters appeared when between-subject variability

far exceeded within-subject variability, reflecting the fact that out-of-sample prediction for a new subject is especially difficult in these cases.

The NCPF sensors presently tested have other uses in addition to the prediction of ambulatory vGRF. For example, the NCPF sensors have previously been used to measure vibrations for machinery bushings [62] and impact energy and forces in American football [63]. When deformed, the NCPF sensors produce a voltage related to the magnitude of impact. These voltages can be measured by connecting the foam to a microcontroller powered by a 3.7 V, 300 mA, lithium ion polymer battery. The NCPF sensors cost approximately $4 per shoe. The electronics cost approximately $50, but this cost depends upon quantity and will decrease with larger numbers of production. Together, the NCPF sensors, microcontroller, and battery increase the weight of the shoe by 25.5 grams, which is substantially less massive than other wearable vGRF measurement systems. The NCPF self-sensing material is made of a combination of 1 mm chopped nickel coated carbon fiber, nickel powder, and Poron® microcellular urethane.

This is the first report concerning the ability of the novel NCPF sensors to predict running vGRF characteristics and the present results are limited in several important ways that have not yet been discussed. The system tested herein, including the novel sensors, accelerometer, and electronics used to measure and record the related signals contained inherent limitations. Although we did not quantify the quality of the electrical connections between each novel sensor and microcontroller, we suspect that the quality of these connections varied and likely decreased prediction accuracies of the general across-subjects models. Further, the low accelerometer sampling rate and few available shoe sizes limit the present results. The low sampling rate of the acceleration data (16 Hz) was due to user error: a setting on the accelerometer was unknowingly set to the undesirably low sampling rate. Additionally, the

NCPF sensors relied on each individual connection made in the lab; future NCPF sensors will be connected to the microcontroller via a printed flexible circuit. It is unclear how/if these improvements will affect accuracy of future vGRF predictions. Another primary limitation of this study is that only young and healthy subjects were tested. It is unclear how/if the present models relate to subjects with characteristics that differ from the present subjects, like obese, aged, injured, or diseased subjects; it will be important to clarify this issue, as the use of these sensors to measure ambulatory vGRF will be particularly valuable for aged, diseased, or otherwise impaired individuals. It is also unclear how the NCPF sensor outputs will behave under various conditions within real-world environments like a moist, sloped, dirt, running surface. Additionally, it is unclear how the present prediction models will fare as the mechanical properties of the sensors change due to degradation of the foam; e.g., over a 3 hour marathon, or the average running shoe life of approximately 500 Km. Additional research is certainly needed to clarify all of these issues.

In summary, this experiment was conducted to evaluate the effectiveness of a new technology, piezoresponsive foam, in predicting specific characteristics of vGRF during running. vGRF were measured at three different running speeds while subjects wore shoes instrumented with NCPF sensors and a triaxial accelerometer. Principal component regression was used to create prediction models from signals originating from the NCPF sensors and accelerometer to predict the vGRF characteristics of interest. For each response variable of interest, the most accurate models were subject-specific models. General models were also created that applied to all subjects within the present study, as well as future subjects that fit within the demographic characteristics of the present sample. Peak vGRF, impulse due to vGRF, and ground contact time were most accurately predicted. Such predictions can be used to reduce running-related injuries

and/or improve running technique and performance. Future research designed to test the effectiveness of future iterations of the novel NCPF sensors and improved data collection systems will build upon the prediction models produced in this study. The purpose of this line of research will continue to be to improve our present ability to predict real-world running vGRF outside of the traditional biomechanics laboratory.

Table 1. Means, standard deviations, and coefficients of variation for six vertical ground reaction force (vGRF) characteristics during running at three different speeds, measured using a force instrumented treadmill, including the percentage of running strides that involved a heel strike pattern.

	2.68 m/s	**3.13 m/s**	**3.58 m/s**
Active Peak vGRF (N)	1584 ± 264	1667 ± 287	1742 ± 298
Coefficient of Variation (%)	17	17	17
Impulse (Ns)	254 ± 42	249 ± 42	247 ± 42
Coefficient of Variation (%)	17	17	17
Ground Contact Time (s)	0.268 ± 0.015	0.248 ± 0.012	0.232 ± 0.012
Coefficient of Variation (%)	6	5	5
Impact Peak vGRF (N)	923 ± 195	1073 ± 232	1278 ± 270
Coefficient of Variation (%)	21	22	21
Average Impact Rate (KN/s)	36.2 ± 11.0	43.8 ± 12.1	54.9 ± 14.9
Coefficient of Variation (%)	30	28	27
Max Impact Rate (KN/s)	52.3 ± 17.7	63.4 ± 20.9	81.6 ± 25.8
Coefficient of Variation (%)	34	33	32
Percent Heel Strike Pattern	23%	40%	51%

Table 2. Correlation values describing linear relationships between the most highly correlated predictor variables and measured vertical ground reaction force (vGRF) characteristics. Correlations between these predictor variables and measured vGRF characteristics allowed for prediction of vGRF characteristics using novel sensors and an accelerometer attached to a running shoe. (BMI = body mass index; NCPF = novel nanocomposite piezoresponsive foam sensors placed under the arch, ball, or toe; Accel = X, Y, Z, or resultant acceleration measured via an accelerometer placed approximately over the shoelaces)

Active Peak vGRF		Impulse		Ground Contact Time	
Predictor	**Correlation**	**Predictor**	**Correlation**	**Predictor**	**Correlation**
Subject Weight	0.91	Subject Weight	0.95	Z Accel: Integral	-0.56
Subject Height	0.68	Subject Height	0.72	Res Accel: Integral	-0.55
Subject BMI	0.67	Subject BMI	0.7	Z Accel: Min	0.51
Toe NCPF: Max	0.56	Toe NCPF: Min	-0.48	X Accel: Integral	-0.46
Toe NCPF: Min	-0.56	Toe NCPF: Integral	0.47	Stride Time	0.43
Toe NCPF: Integral	0.55	Toe NCPF: Max	0.45	Res Accel: Primary Freq	-0.37
Ball NCPF: Integral	-0.39	Ball NCPF: Min	0.42	Res Accel: Max	-0.37
Ball NCPF: Max Time	-0.38	Ball NCPF: Integral	-0.41	X Accel: Primary Freq	-0.36
Y Accel: Min	-0.37	Y Accel: Min	-0.38	Arch NCPF: Min	0.31
Ball NCPF: Min	0.35	Ground Contact Time	0.35	X Accel: Max	-0.31

Impact Peak vGRF		Average Impact Rate		Maximum Impact Rate	
Predictor	**Correlation**	**Predictor**	**Correlation**	**Predictor**	**Correlation**
Subject Weight	0.75	Subject Weight	0.67	Subject Weight	0.69
Subject BMI	0.62	Ball NCPF: Integral	-0.58	Ball NCPF: Integral	-0.6
Ball NCPF: Integral	-0.6	Subject BMI	0.57	Subject BMI	0.58
Toe NCPF: Min	-0.45	Toe NCPF: Min Time	-0.45	Toe NCPF: Min Time	-0.51
Subject Height	0.44	Toe NCPF: Min	-0.4	Toe NCPF: Min	-0.46
Ball NCPF: Max Time	-0.44	Ball NCPF: Max Time	-0.38	Subject Height	0.39
Toe NCPF: Min Time	-0.43	Y Accel: Integral	0.37	Z Accel: Integral	0.38
Y Accel: Integral	0.42	Z Accel: Integral	0.36	Ball NCPF: Max Time	-0.37
Ball NCPF: Min	0.41	Ball NCPF: Min	0.36	Ball NCPF: Min	0.36
Toe NCPF: Max	0.4	Subject Height	0.36	Y Accel: Integral	0.32

Table 3. Average root mean squared error (RMSE) for the leave-one-subject-out cross-validation analyses of the general (across-subjects) models created in the present study, and some information concerning each model (i.e., which demographic predictor variables were used, and how many novel sensor and acceleration predictor variables were used). RMSE for active peak vertical ground reaction force (vGRF) magnitude, impulse due to vGRF, and ground contact time were relatively low, while errors for impact peak vGRF and corresponding average and maximum instantaneous load rates were greater. (G = gender; W = body weight; B = body mass index; A = age; H = height)

vGRF Characteristic	Leave-one-subject-out Mean RMSE (% Error)	Demographic Variables Used	# of Used Sensor Variables	# of Used Principal Components
Active Peak vGRF (N)	129.8 (6.87%)	G, W, B	7	9
Impulse (N*s)	17.69 (6.67%)	W, B	10	11
Ground Contact Time (s)	0.0171 (5.77%)	A, G, W, H, B	7	10
Impact Peak vGRF (N)	316.94 (26.09%)	G, W	8	8
Average Impact Rate (kN/s)	10.544 (28.85%)	W	7	7
Max Impact Rate (kN/s)	14.987 (25.04%)	W	4	5

Table 4. Average root mean squared errors (RMSE; i.e., actual minus predicted) for the subject-specific models created using 30, 50, and 70%, of each subject's data as the training data. Active peak vertical ground reaction force (vGRF) magnitude, impulse due to vGRF, and ground contact time errors were relatively low, while errors for impact peak vGRF and corresponding average and maximum instantaneous load rates were greater.

	Percent of Data Used to Train the Model		
vGRF Characteristic	**30%**	**50%**	**70%**
Active Peak vGRF (N)	59.4 (2.9%)	59.0 (2.9%)	60.4 (3.0%)
Impulse (N*s)	5.8 (1.9%)	5.4 (1.7%)	5.1 (1.6%)
Ground Contact Time (s)	0.011 (3.4%)	0.011 (3.6%)	0.011 (3.6%)
Impact Peak vGRF (N)	131.6 (9.4%)	122.7 (8.8%)	123.0 (8.8%)
Average Impact Rate (kN/s)	8.8 (26.7%)	8.5 (25.5%)	8.2 (26.5%)
Max Impact Rate (kN/s)	12.9 (24.0%)	11.4 (22.1%)	11.1 (22.2%)

Figure 1. A typical vertical ground reaction force curve observed during the present study. The following characteristics of the curve were predicted via novel piezoresponsive sensors and an accelerometer attached to the running shoe: impact and active peak magnitudes, average impact peak load rate (depicted via the slope of the dashed line), maximum instantaneous impact peak load rate, ground contact time (depicted via the length of the dotted line), and impulse due to the ground reaction force.

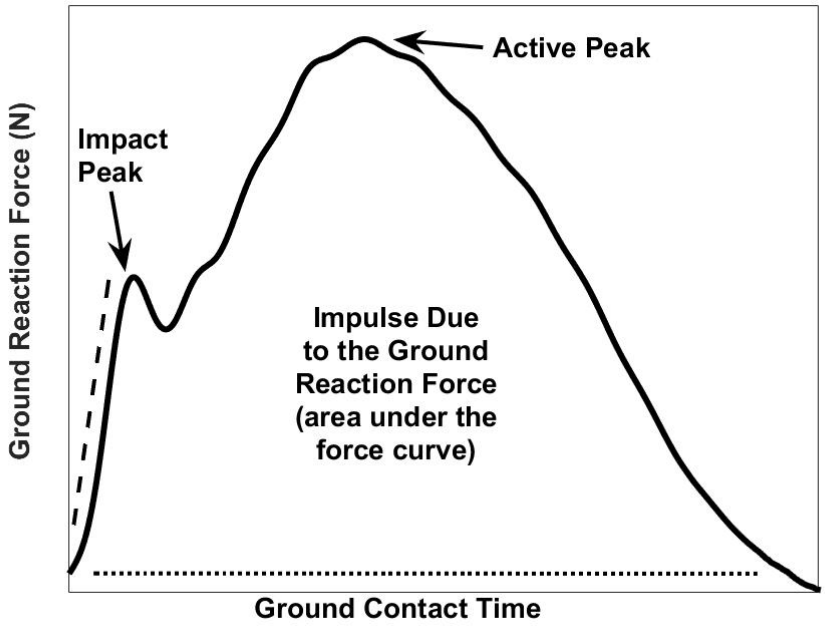

Figure 2. The running shoes used throughout the present study were instrumented with four novel nanocomposite piezoresponsive foam sensors (2A) and a triaxial accelerometer (2B).

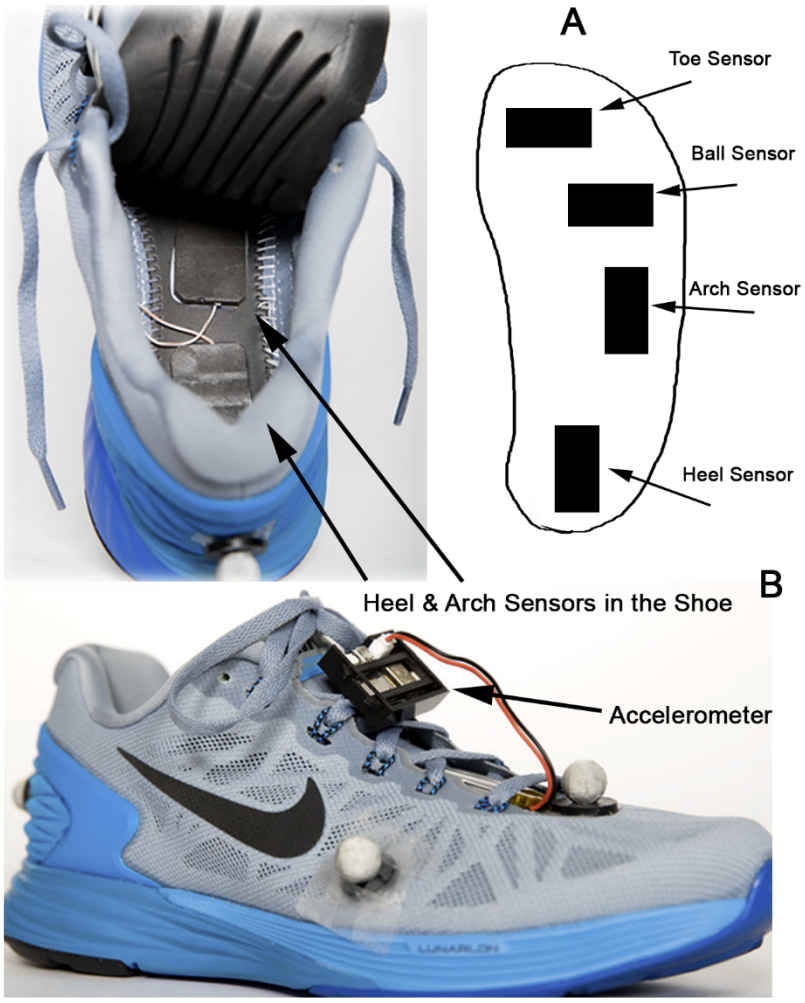

Figure 3. Ten representative vertical ground reaction force (GRF) traces measured using a force instrumented treadmill from three different running speeds, for three different subjects. Subjects 302 and 340 exhibited primarily heel-strike patterns, while Subject 320 exhibited primarily non-heel-strike patterns.

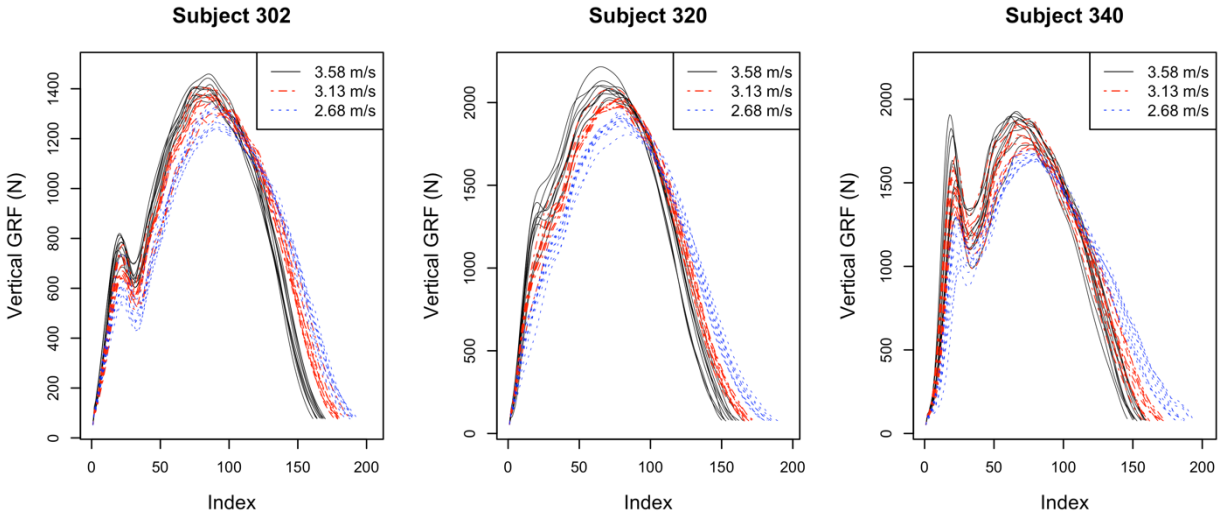

Figure 4. Out-of-sample predicted values from the cross-validation process on the general (across-all-subjects) model vs. actual measurements of each of the six quantitative variables of interest. Predictions are closest to actual values for the impulse and active peak vGRF variables. Overall bias is small across all actual measured values for each of the variables of interest.

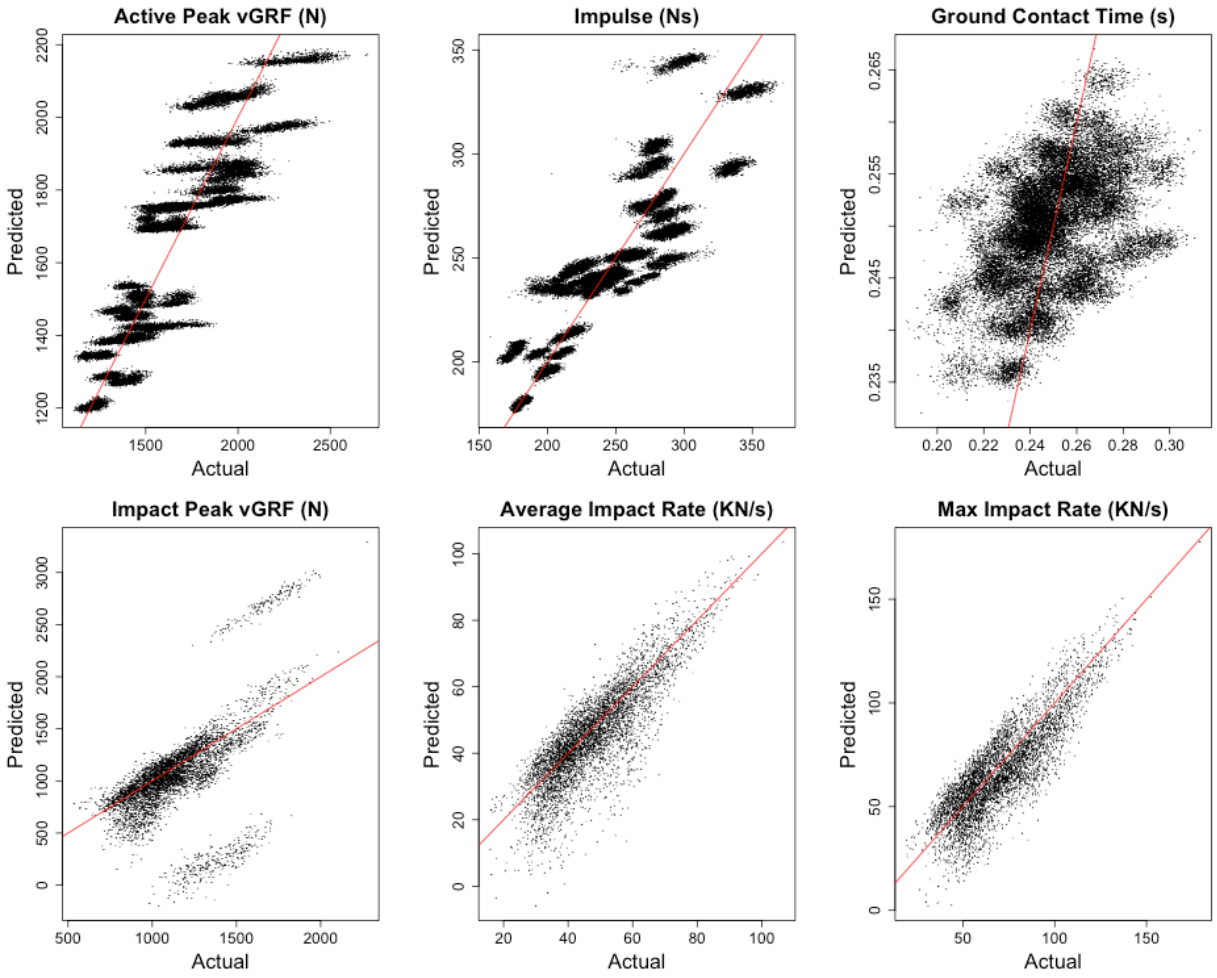

Appendix A. An explanation of all of the predictor variables used in the final general models (across-all-subjects) to predict each of the seven vertical ground reaction force (vGRF) characteristics (response variables) of interest. For example, the model for the response variable "Active Peak vGRF" used 7 of the possible 48 sensor-based predictors including: (1) max on the Z Accel curve, (2) primary frequency on the Z Accel curve, (3) max on the Resultant Accel curve,…, and (7) max on the NCPF Toe curve. The model for "Active Peak vGRF" also used Gender, Weight, and BMI. Subject weight was the most used predictor variable. The novel nanocomposite piezoresponsive foam (NCPF) sensors placed under the heel and ball of the foot were used more often than sensors placed under the arch and toe.

	Active Peak vGRF						Impulse						Stance Duration						Peak Impact Force						Avg Impact Rate						Max Impact Rate						Foot-Strike Pattern					
	Max	Time to Max	Min	Time to Min	Time Integral	Primary Frequency	Max	Time to Max	Min	Time to Min	Time Integral	Primary Frequency	Max	Time to Max	Min	Time to Min	Time Integral	Primary Frequency	Max	Time to Max	Min	Time to Min	Time Integral	Primary Frequency	Max	Time to Max	Min	Time to Min	Time Integral	Primary Frequency	Max	Time to Max	Min	Time to Min	Time Integral	Primary Frequency	Max	Time to Max	Min	Time to Min	Time Integral	Primary Frequency
X Accel.								X													X	X																	X		X	
Y Accel.								X												X							X		X													
Z Accel.	X					X		X	X		X	X					X											X						X								
Res. Accel	X												X				X						X																		X	
Heel			X						X				X		X						X						X		X				X						X			
Arch			X								X																												X			
Ball		X							X					X					X		X		X				X		X				X									
Toe	X																																				X					
Stride Duration									X						X																											
Demographics	Age	Gender	Weight	Height	BMI		Age	Gender	Weight	Height	BMI		Age	Gender	Weight	Height	BMI		Age	Gender	Weight	Height	BMI		Age	Gender	Weight	Height	BMI		Age	Gender	Weight	Height	BMI		Age	Gender	Weight	Height	BMI	
		X	X		X				X		X		X	X	X	X	X			X	X						X						X									

Appendix B. Additional descriptive data for each of the final general models (across-all-subjects) used to predict various discrete characteristics of running vertical ground reaction force. Coefficients and standard errors are standardized on the scale of the covariates.

Active Peak vGRF (N)

	Estimate	Standard Error	t value	Lower 95% Bound	Upper 95% Bound
(Intercept)	1665.020	13.470	123.630	1638.620	1691.410
Subject Weight	106.900	5.850	18.290	95.440	118.360
Toe NCPF: Max	7.760	0.880	8.850	6.040	9.480
Res Accel: Integral	5.110	0.510	9.930	4.100	6.120
Subject Gender	105.060	13.000	8.080	79.570	130.550
Heel NCPF: Min	-4.250	1.170	-3.620	-6.550	-1.940
Res Accel: Max	-8.090	0.670	-12.140	-9.400	-6.790
Z Accel: Max	2.870	0.510	5.630	1.870	3.860
Subject BMI	84.620	11.190	7.560	62.680	106.560
Z Accel: Primary Freq	1.080	0.290	3.740	0.510	1.640
Arch NCPF: Max	14.400	0.860	16.670	12.710	16.090
R.squared: 0.80					
F-statistic: 109.9 (9, 28623 df)					
AR(1) Coefficient: 0.41					
SD Random Intercept: 126.98					

Impulse due to vGRF (Ns)

	Estimate	Standard Error	t value	Lower 95% Bound	Upper 95% Bound
(Intercept)	250.510	2.110	118.480	246.370	254.650
Subject Weight	17.260	1.000	17.240	15.300	19.230
Stride Time	2.110	0.060	34.820	1.990	2.230
Z Accel: Integral	-1.260	0.060	-19.840	-1.380	-1.130
Heel NCPF: Min	-2.630	0.130	-20.540	-2.880	-2.380
Subject BMI	20.230	1.210	16.670	17.850	22.610
Arch NCPF: Integral	-1.080	0.190	-5.620	-1.450	-0.700
Z Accel: Primary Freq	0.380	0.030	12.860	0.320	0.440
X Accel: Max Time	-0.330	0.020	-13.480	-0.380	-0.280
Z Accel: Max Time	0.160	0.020	6.460	0.110	0.210
Z Accel: Min	1.140	0.080	15.010	0.990	1.290
Y Accel: Max Time	-0.090	0.030	-2.620	-0.160	-0.020
Ball NCPF: Min	0.970	0.120	8.400	0.750	1.200
R.squared: 0.78					
F-statistic: 242.0 (11, 28621 df)					
AR(1) Coefficient: 0.47					
SD Random Intercept: 19.94					

Ground Contact Time (s)

	Estimate	Standard Error	t value	Lower 95% Bound	Upper 95% Bound
(Intercept)	0.24984	0.00169	147.49420	0.24652	0.25316
Z Accel: Integral	-0.00042	0.00011	-3.91123	-0.00063	-0.00021
Stride Time	0.00198	0.00010	19.46941	0.00178	0.00217
Subject Weight	0.00176	0.00075	2.34633	0.00029	0.00323
Ball NCPF: Max Time	0.00018	0.00005	3.76488	0.00009	0.00028
Res Accel: Integral	-0.00233	0.00017	-13.49891	-0.00267	-0.00199
Res Accel: Max	0.00057	0.00006	9.29148	0.00045	0.00069
Subject Age	0.00138	0.00177	0.78331	-0.00208	0.00485
Subject Gender	-0.00090	0.00074	-1.22025	-0.00236	0.00055
Heel NCPF: Min	0.00060	0.00016	3.70757	0.00028	0.00092
Subject Height	0.00334	0.00109	3.05575	0.00120	0.00548
Subject BMI	-0.00022	0.00129	-0.16752	-0.00274	0.00231
Heel NCPF: Max	-0.00052	0.00010	-5.46341	-0.00071	-0.00034
R.squared: 0.28					
F-statistic: 58.3 (10, 28622 df)					
AR(1) Coefficient: 0.37					
SD Random Intercept: 0.02					

Peak Impact Force (N)

	Estimate	Standard Error	t value	Lower 95% Bound	Upper 95% Bound
(Intercept)	1100.740	21.668	50.801	1058.270	1143.209
Subject Weight	22.738	19.155	1.187	-14.806	60.283
Ball NCPF: Integral	-70.376	6.110	-11.518	-82.353	-58.400
Res Accel: Integral	-0.952	1.362	-0.699	-3.622	1.718
Ball NCPF: Min	-7.466	1.802	-4.144	-10.997	-3.935
Heel NCPF: Min	-70.090	3.162	-22.167	-76.287	-63.892
Subject Gender	141.449	13.346	10.598	115.290	167.609
Ball NCPF: Max	14.357	2.114	6.790	10.213	18.501
Y Accel: Max Time	-1.596	1.082	-1.476	-3.717	0.524
X Accel: Min	2.110	1.105	1.909	-0.057	4.276
X Accel: Min Time	1.792	0.889	2.015	0.049	3.535
R.squared: 0.62					
F-statistic: 77.7 (8, 10714 df)					
AR(1) Coefficient: 0.17					
SD Random Intercept: 183.16					

Average Load Rate (kN/s)

	Estimate	Standard Error	t value	Lower 95% Bound	Upper 95% Bound
(Intercept)	44.074	1.026	42.950	42.063	46.085
Subject Weight	7.456	0.862	8.647	5.766	9.146
Ball NCPF: Integral	-3.580	0.263	-13.617	-4.095	-3.065
Ball NCPF: Min	-3.133	0.182	-17.178	-3.490	-2.775
Heel NCPF: Min	-5.699	0.260	-21.949	-6.208	-5.190
Y Accel: Integral	0.797	0.156	5.100	0.490	1.103
Z Accel: Integral	0.347	0.095	3.640	0.160	0.535
Heel NCPF: Integral	-4.834	0.308	-15.711	-5.437	-4.231
Y Accel: Min	-0.405	0.156	-2.596	-0.711	-0.099
R.squared: 0.57					
F-statistic: 129.5 (7, 10715 df)					
AR(1) Coefficient: 0.24					
SD Random Intercept: 8.58					

Maximum Instantaneous Load Rate (kN/s)

	Estimate	Standard Error	t value	Lower 95% Bound	Upper 95% Bound
(Intercept)	63.774	1.447	44.083	60.938	66.609
Subject Weight	12.985	1.224	10.610	10.587	15.384
Ball NCPF: Integral	-14.708	0.737	-19.962	-16.153	-13.264
Ball NCPF: Min	-7.619	0.299	-25.518	-8.205	-7.034
Heel NCPF: Min	-5.013	0.332	-15.117	-5.663	-4.363
Z Accel: Integral	0.516	0.119	4.325	0.282	0.749
R.squared: 0.70					
F-statistic: 259.5 (5, 10717 df)					
AR(1) Coefficient: 0.30					
SD Random Intercept: 12.07					

Funding Details

This research was supported by the National Science Foundation: Grant Numbers: CMMI-XXXX & CMMI-XXXX.

Disclosure of Interests

XXXX, XXXX, and XXXX are listed inventors on the patent for the nanocomposite piezo-responsive foam (NCPF) sensors discussed in this paper. XXXX is the majority owner of Nano Composite Products, which has licensed the patents related to the technology presented in this paper from XXXX.

References

[1] Running and Jogging - Statistics and Facts. https://www.statista.com/topics/1743/running-and-jogging/, 2019 (accessed March 13 2019).
[2] P. Schnohr, J.L. Marott, P. Lange, G.B. Jensen, Longevity in Male and Female Joggers: The Copenhagen City Heart Study, American Journal of Epidemiology 177(7) (2013) 683-689. http://dx.doi.org/10.1093/aje/kws301.
[3] D.-c. Lee, R.R. Pate, C.J. Lavie, X. Sui, T.S. Church, S.N. Blair, Leisure-Time Running Reduces All-Cause and Cardiovascular Mortality Risk, Journal of the American College of Cardiology 64(5) (2014) 472. http://www.onlinejacc.org/content/64/5/472.abstract.
[4] A. Boudenot, Z. Achiou, H. Portier, Does running strengthen bone?, Applied physiology, nutrition, and metabolism = Physiologie appliquee, nutrition et metabolisme 40(12) (2015) 1309-12.
[5] B. Winter, C. Breitenstein, F.C. Mooren, K. Voelker, M. Fobker, A. Lechtermann, et al., High impact running improves learning, Neurobiology of Learning and Memory 87(4) (2007) 597-609. http://www.sciencedirect.com/science/article/pii/S1074742706001596.
[6] R.D. Hyldahl, A. Evans, S. Kwon, S.T. Ridge, E. Robinson, J.T. Hopkins, et al., Running decreases knee intra-articular cytokine and cartilage oligomeric matrix concentrations: a pilot study, European journal of applied physiology 116(11-12) (2016) 2305-2314.
[7] Z.H. Lewis, E.J. Lyons, J.M. Jarvis, J. Baillargeon, Using an electronic activity monitor system as an intervention modality: A systematic review, BMC public health 15 (2015) 585.
[8] K.M. Polzien, J.M. Jakicic, D.F. Tate, A.D. Otto, The efficacy of a technology-based system in a short-term behavioral weight loss intervention, Obesity 15(4) (2007) 825-830.
[9] F.A. Barwais, T.F. Cuddihy, L.M. Tomson, Physical activity, sedentary behavior and total wellness changes among sedentary adults: a 4-week randomized controlled trial, Health and quality of life outcomes 11(1) (2013) 183.
[10] P.G. Weyand, D.B. Sternlight, M.J. Bellizzi, S. Wright, Faster top running speeds are achieved with greater ground forces not more rapid leg movements, Journal of applied physiology (Bethesda, Md. : 1985) 89(5) (2000) 1991-9.
[11] K.L. Popp, W. McDermott, J.M. Hughes, S.A. Baxter, S.D. Stovitz, M.A. Petit, Bone strength estimates relative to vertical ground reaction force discriminates women runners with stress fracture history, Bone 94 (2017) 22-28.
[12] C.E. MILNER, R. FERBER, C.D. POLLARD, J. HAMILL, I.S. DAVIS, Biomechanical Factors Associated with Tibial Stress Fracture in Female Runners, Medicine & Science in Sports & Exercise 38(2) (2006) 323-328. https://journals.lww.com/acsm-msse/Fulltext/2006/02000/Biomechanical_Factors_Associated_with_Tibial.19.aspx.
[13] J. Bigouette, J. Simon, K. Liu, C.L. Docherty, Altered Vertical Ground Reaction Forces in Participants With Chronic Ankle Instability While Running, Journal of athletic training 51(9) (2016) 682-687.
[14] M.B. Pohl, D.R. Mullineaux, C.E. Milner, J. Hamill, I.S. Davis, Biomechanical predictors of retrospective tibial stress fractures in runners, Journal of biomechanics 41(6) (2008) 1160-5.
[15] A.A. Zadpoor, A.A. Nikooyan, The relationship between lower-extremity stress fractures and the ground reaction force: a systematic review, Clinical biomechanics (Bristol, Avon) 26(1) (2011) 23-8.

[16] I.S. Davis, B.J. Bowser, D.R. Mullineaux, Greater vertical impact loading in female runners with medically diagnosed injuries: a prospective investigation, British Journal of Sports Medicine 50(14) (2016) 887. http://bjsm.bmj.com/content/50/14/887.abstract.
[17] C.E. Milner, R. Ferber, C.D. Pollard, J. Hamill, I.S. Davis, Biomechanical factors associated with tibial stress fracture in female runners, Med. Sci. Sports Exerc. 38(2) (2006) 323-8.
[18] M.B. Pohl, J. Hamill, I.S. Davis, Biomechanical and anatomic factors associated with a history of plantar fasciitis in female runners, Clinical journal of sport medicine : official journal of the Canadian Academy of Sport Medicine 19(5) (2009) 372-6.
[19] H. van der Worp, J.W. Vrielink, S.W. Bredeweg, Do runners who suffer injuries have higher vertical ground reaction forces than those who remain injury-free? A systematic review and meta-analysis, British Journal of Sports Medicine 50(8) (2016) 450. http://bjsm.bmj.com/content/50/8/450.abstract.
[20] A. Nummela, T. Keranen, L.O. Mikkelsson, Factors related to top running speed and economy, International journal of sports medicine 28(8) (2007) 655-61.
[21] R.F. Chapman, A.S. Laymon, D.P. Wilhite, J.M. McKenzie, D.A. Tanner, J.M. Stager, Ground contact time as an indicator of metabolic cost in elite distance runners, Medicine and science in sports and exercise 44(5) (2012) 917-25.
[22] T.J. Roberts, R. Kram, P.G. Weyand, C.R. Taylor, Energetics of bipedal running. I. Metabolic cost of generating force, The Journal of experimental biology 201(Pt 19) (1998) 2745-51.
[23] M. Chan-Roper, J. Hunter I Fau - W Myrer, D. W Myrer J Fau - L Eggett, M. L Eggett D Fau - K Seeley, K.S. M, Kinematic changes during a marathon for fast and slow runners, (1303-2968 (Print)).
[24] J. Petersen, H. Sorensen, R.O. Nielsen, Cumulative loads increase at the knee joint with slow-speed running compared to faster running: a biomechanical study, The Journal of orthopaedic and sports physical therapy 45(4) (2015) 316-22.
[25] R.H. Miller, Joint Loading in Runners Does Not Initiate Knee Osteoarthritis, Exercise and sport sciences reviews 45(2) (2017) 87-95.
[26] R.H. Miller, W.B. Edwards, S.C. Brandon, A.M. Morton, K.J. Deluzio, Why don't most runners get knee osteoarthritis? A case for per-unit-distance loads, Medicine and science in sports and exercise 46(3) (2014) 572-9.
[27] M.A. Brodie, M.J. Coppens, S.R. Lord, N.H. Lovell, Y.J. Gschwind, S.J. Redmond, et al., Wearable pendant device monitoring using new wavelet-based methods shows daily life and laboratory gaits are different, Medical & biological engineering & computing 54(4) (2016) 663-74.
[28] J.A. Garcia-Perez, P. Perez-Soriano, S. Llana Belloch, A.G. Lucas-Cuevas, D. Sanchez-Zuriaga, Effects of treadmill running and fatigue on impact acceleration in distance running, Sports biomechanics 13(3) (2014) 259-66.
[29] B. Kluitenberg, S.W. Bredeweg, S. Zijlstra, W. Zijlstra, I. Buist, Comparison of vertical ground reaction forces during overground and treadmill running. A validation study, BMC musculoskeletal disorders 13(1) (2012) 235.
[30] J.H. Challis, The Variability in Running Gait Caused by Force Plate Targeting, Journal of Applied Biomechanics 17(1) (2001) 77-83. https://doi.org/10.1123/jab.17.1.77.
[31] A. Ancillao, S. Tedesco, J. Barton, B. O'Flynn, Indirect Measurement of Ground Reaction Forces and Moments by Means of Wearable Inertial Sensors: A Systematic Review, Sensors (Basel, Switzerland) 18(8) (2018).

[32] K.J. Ngoh, D. Gouwanda, A.A. Gopalai, Y.Z. Chong, Estimation of vertical ground reaction force during running using neural network model and uniaxial accelerometer, Journal of biomechanics 76 (2018) 269-273.
[33] E. Shahabpoor, A. Pavic, Estimation of vertical walking ground reaction force in real-life environments using single IMU sensor, Journal of biomechanics 79 (2018) 181-190. http://www.sciencedirect.com/science/article/pii/S0021929018306821.
[34] E. Shahabpoor, A. Pavic, J.M.W. Brownjohn, S.A. Billings, L.Z. Guo, M. Bocian, Real-Life Measurement of Tri-Axial Walking Ground Reaction Forces Using Optimal Network of Wearable Inertial Measurement Units, IEEE transactions on neural systems and rehabilitation engineering : a publication of the IEEE Engineering in Medicine and Biology Society 26(6) (2018) 1243-1253.
[35] W. Seiberl, E. Jensen, J. Merker, M. Leitel, A. Schwirtz, Accuracy and precision of loadsol((R)) insole force-sensors for the quantification of ground reaction force-based biomechanical running parameters, European journal of sport science 18(8) (2018) 1100-1109.
[36] M. Koch, L.K. Lunde, M. Ernst, S. Knardahl, K.B. Veiersted, Validity and reliability of pressure-measurement insoles for vertical ground reaction force assessment in field situations, Applied ergonomics 53 Pt A (2016) 44-51.
[37] T. Stoggl, A. Martiner, Validation of Moticon's OpenGo sensor insoles during gait, jumps, balance and cross-country skiing specific imitation movements, Journal of sports sciences 35(2) (2017) 196-206.
[38] D.A. Jacobs, D.P. Ferris, Estimation of ground reaction forces and ankle moment with multiple, low-cost sensors, Journal of neuroengineering and rehabilitation 12 (2015) 90.
[39] D.E. Lieberman, M. Venkadesan, W.A. Werbel, A.I. Daoud, S. D'Andrea, I.S. Davis, et al., Foot strike patterns and collision forces in habitually barefoot versus shod runners, Nature 463 (2010) 531. https://doi.org/10.1038/nature08723.
[40] C.A. Laughton, I.M. Davis, J. Hamill, Effect of strike pattern and orthotic intervention on tibial shock during running, Journal of applied biomechanics 19(2) (2003) 153-168.
[41] P.G. Rosquist, G. Collins, A.J. Merrell, N.J. Tuttle, J.B. Tracy, E.T. Bird, et al., Estimation of 3D Ground Reaction Force Using Nanocomposite Piezo-Responsive Foam Sensors During Walking, Annals of biomedical engineering 45(9) (2017) 2122-2134.
[42] E.L. Radin, M.W. Whittle, K.H. Yang, R.J. Jefferson, M.M. Rodgers, V.L. Kish, et al., HEELSTRIKE TRANSIENT, ITS RELATIONSHIP WITH THE ANGULAR VELOCITY OF THE SHANK AND THE EFFECTS OF QUADRICEPS PARALYSIS, 1986, pp. 121-123.
[43] M.H. Kutner, Applied Linear Statistical Models, McGraw-Hill Irwin2005.
[44] S. Weisberg, Applied Linear Regression, Wiley2013.
[45] G. James, D. Witten, T. Hastie, R. Tibshirani, An Introduction to Statistical Learning: with Applications in R, Springer2013.
[46] N.R. Draper, H. Smith, Applied Regression Analysis, Wiley1981.
[47] R.H. Myers, Classical and modern regression with applications, 2nd ed. ed., Boston (Mass.) : PWS-KENT1990.
[48] P. Diggle, D.M.S.P.J. Diggle, F.a. tierzucht, O.U. Press, P.J. Diggle, P. Heagerty, et al., Analysis of Longitudinal Data, OUP Oxford2002.
[49] N. Chambon, N. Delattre, N. Guéguen, E. Berton, G. Rao, Shoe drop has opposite influence on running pattern when running overground or on a treadmill, European journal of applied physiology 115(5) (2015) 911-918.

[50] B.M. Nigg, R.W. De Boer, V. Fisher, A kinematic comparison of overground and treadmill running, Medicine and science in sports and exercise 27(1) (1995) 98-105.
[51] K.E. Gerlach, S.C. White, H.W. Burton, J.M. Dorn, J.J. Leddy, P.J. Horvath, Kinetic changes with fatigue and relationship to injury in female runners, Medicine and science in sports and exercise 37(4) (2005) 657-63.
[52] M. Anbarian, H. Esmaeili, Effects of running-induced fatigue on plantar pressure distribution in novice runners with different foot types, Gait & posture 48 (2016) 52-56.
[53] D.L. Headlee, J.L. Leonard, J.M. Hart, C.D. Ingersoll, J. Hertel, Fatigue of the plantar intrinsic foot muscles increases navicular drop, Journal of electromyography and kinesiology : official journal of the International Society of Electrophysiological Kinesiology 18(3) (2008) 420-5.
[54] K.H. Schutte, S. Seerden, R. Venter, B. Vanwanseele, Influence of outdoor running fatigue and medial tibial stress syndrome on accelerometer-based loading and stability, Gait & posture 59 (2018) 222-228.
[55] K.A. Valenzuela, S.K. Lynn, L.R. Mikelson, G.J. Noffal, D.A. Judelson, Effect of Acute Alterations in Foot Strike Patterns during Running on Sagittal Plane Lower Limb Kinematics and Kinetics, (1303-2968 (Print)).
[56] J. Bigouette, J. Simon, K. Liu, C.L. Docherty, Altered Vertical Ground Reaction Forces in Participants With Chronic Ankle Instability While Running, (1938-162X (Electronic)).
[57] B.J. Bowser, R. Fellin, C.E. Milner, M.B. Pohl, I.S. Davis, Reducing Impact Loading in Runners: A One-Year Follow-up, Medicine and science in sports and exercise 50(12) (2018) 2500-2506.
[58] F.J. Wouda, M. Giuberti, G. Bellusci, E. Maartens, J. Reenalda, B.F. van Beijnum, et al., Estimation of Vertical Ground Reaction Forces and Sagittal Knee Kinematics During Running Using Three Inertial Sensors, Frontiers in physiology 9 (2018) 218.
[59] H. Rouhani, J. Favre, X. Crevoisier, K. Aminian, Ambulatory assessment of 3D ground reaction force using plantar pressure distribution, Gait Posture. 32(3) (2010) 311-6. doi: 10.1016/j.gaitpost.2010.05.014. Epub 2010 Jun 23.
[60] H.H. Savelberg, A.L. de Lange, novel Award Third Prize Paper. Assessment of the horizontal,fore-aft component of the ground reaction force from insole pressure patterns by using artificial neural networks, Clin Biomech (Bristol, Avon). 14(8) (1999) 585-92. doi: 10.1016/s0268-0033(99)00036-4.
[61] R. Eguchi, A. Yorozu, T. Fukumoto, M. Takahashi, Estimation of Vertical Ground Reaction Force Using Low-cost Insole with Force Plate-free Learning from Single Leg Stance and Walking, IEEE J Biomed Health Inform 23(10) (2019) 2937279.
[62] E.T. Bird, A.J. Merrell, B.K. Anderson, C.N. Newton, P.G. Rosquist, D.T. Fullwood, et al., Vibration monitoring via nano-composite piezoelectric foam bushings, Smart Materials and Structures 25(11) (2016) 115013. http://dx.doi.org/10.1088/0964-1726/25/11/115013.
[63] A.J. Merrell, W.F. Christensen, M.K. Seeley, A.E. Bowden, D.T. Fullwood, Nano-Composite Foam Sensor System in Football Helmets, Annals of biomedical engineering 45(12) (2017) 2742-2749.